EARTH SCIENCES
RESEARCH JOURNAL

Earth Sci. Res. J. Vol. 24, No. 1 (March, 2020): 45-54

UNIVERSIDAD NACIONAL DE COLOMBIA

GEOLOGICAL ENGINEERING

Evolution Laws of Floor Stress and Stability of Floor Roadway Affected by Overhead Mining

Pu Wang[1], Lishuai Jiang[1]*, Changqing Ma[1], Anying Yuan[2]
[1]Department of Resources and Civil Engineering, Shandong University of Science and Technology, Tai'an, 271019, China
[2]State Key Laboratory of Mining Disaster Prevention and Control co founded by Shandong Province nd the Ministry of Science and Technology, Shandong University of Science and Technology, Qingdao 266590, China
* Corresponding author: skwp0701@hotmail.com

ABSTRACT

Based on the geological conditions of a drainage roadway in the Xinglongzhuang coalmine of Shandong province (China), a mechanical model of a working face for overhead mining over a roadway was established, and the laws influencing the mining-induced stress were obtained. The evolution of mining-induced stress in the floor with different horizontal distances between working face and floor roadway was examined using universal distinct element code (UDEC) numerical simulation; the stability of the floor roadway was analyzed. The results of the numerical simulation were verified via on-site tests of the deformation of surrounding rocks and bolt pull-out readings from the drainage roadway. The results indicated that the floor roadway was significantly affected within a certain depth and then the effect weakened with the depth increasing. In view of the roadway stability, the roadway was observed with worse stability of surrounding rocks during the period of the working face mining near the roadway or just passing the roadway; moreover, this exploitation was not safe and needed to strengthen the support for the roadway. The results may provide a scientific basis for determining reasonable locations and support for roadways in Xinglongzhuang coalmine and other coal mines with similar coal measures strata.

Keywords: Overhead mining; floor roadway; mining-induced stress; roadway stability.

Leyes de evolución en el esfuerzo del suelo y de estabilidad de la superficie de una calzada afectada por minería aérea

RESUMEN

Este artículo estableció un modelo mecánico de un frente de trabajo aéreo sobre una calzada con base en las condiciones geológicas de la calzada de drenaje de la mina de carbón Xinglongzhuang y se obtuvieron los factores determinantes del esfuerzo inducido por la minería. Parte del estudio examinó la evolución del esfuerzo inducido por minería en el suelo con diferentes distancias horizontales entre el frente de trabajo y la superficie de la calzada a través de una simulación numérica basada en el código de elemento distintivo universal (UDEC, del inglés Universal Distinct Element Code). La estabilidad del suelo también fue analizada. Los resultados de la simulación numérica se verificaron a través de pruebas de campo de la deformación de las rocas circundantes y de las muestras de la calzada de drenaje. Los resultados indican que la superficie de la calzada fue afectada significativamente hasta cierta profundiad y luego el efecto se debilitó a medida que la profundidad se incrementa. Los resultados muestran que la estabilidad de la calzada registró el peor índice de las rocas circundantes durante el tiempo en que el frente de trabajo estuvo cerca de la calzada o tuvo que pasar por la calzada; lo que significó que esta explotación no es segura y necesitó el fortalecimiento de los soportes de la calzada. Los resultados podrían proveer una base científica para determinar las ubicaciones razonables y los soportes adecuados para calzadas en la mina Xinglongzhuan y en otras minas de carbón con medidas de capas similares.

Palabras clave: minería aérea; superficie de calzada; esfuerzo inducido por la minería; estabilidad de calzada.

Record
Manuscript received: 24/08/2018
Accepted for publication: 25/10/2019

How to cite item
Wang, P., Jiang, L., Ma, C., & Yuan, A. (2020). Evolution Laws of Floor Stress and Stability of Floor Roadway Affected by Overhead Mining. *Earth Sciences Research Journal*, 24(1), 45-54. DOI: https://doi.org/10.15446/esrj.v24n1.67925

ISSN 1794-6190 e-ISSN 2339-3459

https://doi.org/10.15446/esrj.v24n1.67925

Introduction

Given the increase in the demand for coal, there is an increase in the depth and intensity of mining activities. In order to improve the recovery rate of coal resources and increase their economic benefits, overhead mining technology is widely used. It includes several advantages, such as a low drivage ratio, rational exploitation of resources, and stress-relaxed state for the roadway, and is especially applied to short-distance coal seams and thick coal seams (Kang et al., 2011; Wang et al., 2017).

Coal mining induces a stress readjustment and stress transfer to the deeper part of the floor. Overhead mining significantly affects the floor roadway, and high mining stress concentrates in the surrounding rocks of the roadway to a certain depth, which induces serious deformation such as roof falls, floor heaves, and rib spalling (Wang et al., 2015; Wang et al., 2017; Liu et al., 2017). Several on-site photos of roadway instability are shown in Figure 1.

The stress and deformation of the floor roadway induced by mining activities differ with the position during overhead mining. Hence, it is important to examine the evolution laws of the mining stress on the floor, and the stress distribution and failure of the floor roadway to select the location and roadway parameters.

Several studies have used different methods to focus on the distribution of the mining stress on the floor and the deformation-failure of floor roadway. The stress distribution and its propagation laws on the floor were studied by means of elastic mechanics theory, and the deformation characteristics of surrounding rocks of a floor roadway were obtained (Yin et al., 1992; Yuan et al., 2016). The distribution laws of the mining stress in floor and its additional stress were analyzed by utilizing numerical simulations and physical simulations, and reasonable parameters for a floor roadway layout were obtained (Gao et al., 2015; Ma et al., 2015; Liu et al., 2016; Feng et al., 2016). In terms of the deformation and stability of a roadway, the deformation characteristics of the surrounding rocks, such as the floor heave and roof fall of the roadway, were examined using on-site observations, physical simulations, and numerical simulations (Islam and Shinjo, 2009; Li et al., 2016; Jiang et al., 2016, 2017a). Given the instability of roadways with a soft interlayer, the physical and chemical properties, along with the engineering mechanical properties of the soft interlayer were studied using rock mechanical tests, physical simulations, numerical simulations, and theoretical analysis. Moreover, the instability characteristics and failure mechanism of a roadway with a soft interlayer were analyzed (Li, 2011).

Because of the heterogeneity and anisotropy of the coal measures strata in different coal mines, as well as discrete factors such as interface joints, the commonly used method (i.e., theoretical analysis or empirical formula) can not accurately reflect the engineering problems that we intend to study. Hence, based on the geological conditions of a drainage roadway in Xinglongzhuang coalmine of Shandong province (China), a mechanical model of a working face for overhead mining over the roadway is established. The influence of mining stress on the surrounding rocks of the roadway for different spatial positions of the working face and floor roadway are studied in detail by utilizing a universal distinct element code (UDEC) numerical simulation, and the danger area of the roadway layout under this coal measures strata condition is determined. This may serve as a scientific basis for floor roadway selection, which is affected by overhead mining in Xinglongzhuang coalmine or its surrounding coal mines. It may also provide some roadway support experience and supporting parameters for similar coal measures strata.

Stress analysis of floor roadway affected by overhead mining

Geological conditions of overhead mining

The drainage roadway under coal seam no. 3 of the Shanxi group in the 10th district of the Xinglongzhuang coalmine has a depth of approximately 606 m, which is close to coal seam no. 3. The surrounding rocks are primarily carbonaceous mudstone, and the internal fissures are extremely well developed. Serious damage, including cracking and failure of the surrounding rocks of the roadway, had been induced by the overhead mining of panel 10302, which was in need of repair and support prior to reuse.

Mechanical analysis of floor stress affected by overhead mining

Given the relationship between the advancing direction of working face and floor roadway, the overhead mining was divided into mining with the advancing direction of the working face parallel to the roadway and mining in which the advancing direction was perpendicular to the roadway. Hence, the effects of mining on the floor roadway differed. On-site observations indicated that the mining stress in the surrounding rocks of the floor roadway was affected by overhead mining when the advancing direction perpendicular to the roadway exceeded that of the other type of overhead mining, and the mining influence of the former was more evident (Dai et al., 1999; Yuan et al., 2016). Hence, a mechanical model of overhead mining when the advancing direction was perpendicular to the roadway was established, and the laws influencing the mining stress of a floor roadway with different layers were analyzed.

Front abutment stress can be formed ahead of the coal wall because of the mining activities. In order to solve the problem conveniently, the front abutment stress could be simplified and deemed as a uniform load according to the reference written by Lu et al. (2017). The distribution zone of the front abutment stress approximately corresponded to a rectangle with a length L and width W. The overlying load was viewed as a uniform load q, as illustrated in Figure 2a.

When the peak value of the abutment stress was just above the middle axis of the roadway, the mechanical model was simplified as a plane stress model, as shown in Figure 2b (Dai et al., 1999), and the vertical stress component σ_H of the surrounding rocks of the roadway was obtained as follows:

$$\sigma_H = -\frac{q}{2\pi}\left(4\arctan\frac{L}{H}+\frac{4LH}{L^2+H^2}\right) \quad (1)$$

where q denoted the average value of front abutment stress (MPa); L denoted the length of the working face (m), according to the geological report of the working face, L is 160 m; and σ_H denoted the vertical stress component of surrounding rocks of the roadway (MPa); H denoted the vertical distance between the working face and the floor roadway.

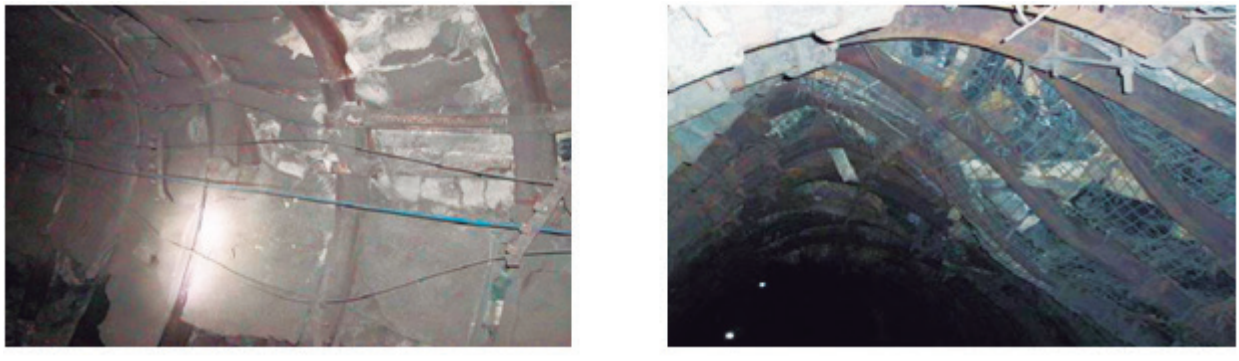

Figure 1. The deformation of the floor roadway is affected by mining activities (Li, 2011).

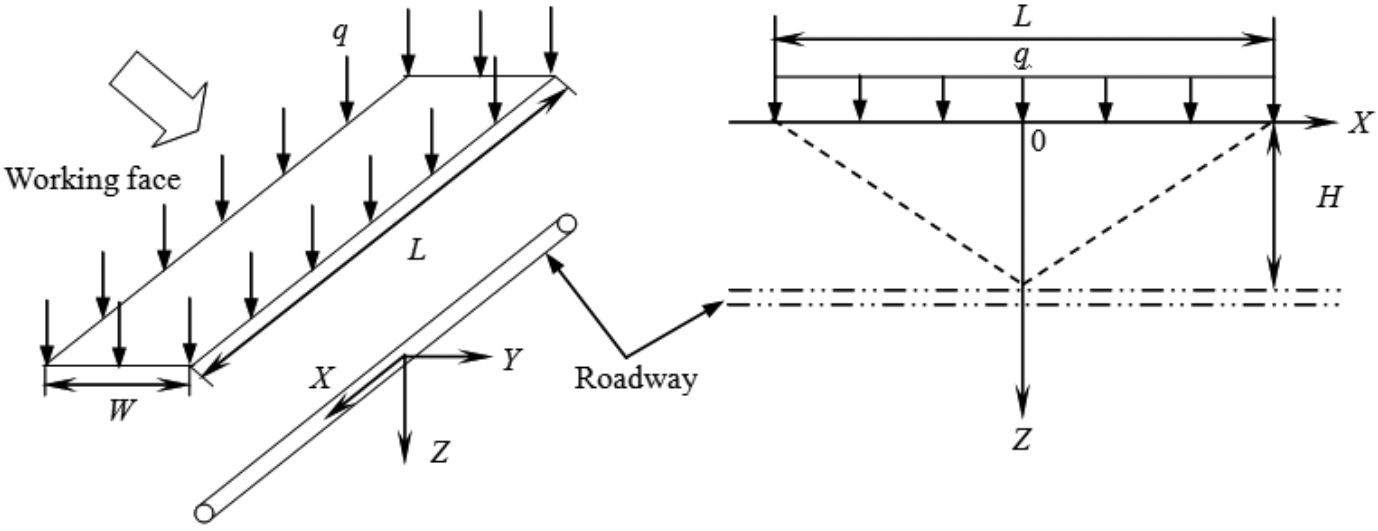

(a) (b)

Figure 2. A mechanical model for overhead mining: (a) spatial model and (b) planar model.

Based on the geological report of the working face, the mining depth h was approximately 566 m. Thus, the in situ stress σ corresponding to level 566 m was calculated by Eq. (2) as follows:

$$\sigma = \gamma h = 25.5\text{kN/m}^3 \times 566\text{m} = 14.43\text{MPa} \quad (2)$$

where γ denoted the unit weight of the rock mass. In the present study, the unit weight of the overlying rock mass was assumed to be 25.5 kN/m3 (Sainoki and Mitri, 2015; Wang et al., 2018). Hence, the average value of the front abutment stress q was 23.09 MPa because the average value of the abutment stress concentration factor was 1.6, as indicated by the geological report of the working face. Thus, the vertical stress σH of the surrounding rocks of the roadway with different positions was calculated by Eq. (1), and the values were listed in Table 1.

Table 1. Vertical stress σ_H of surrounding rocks of the roadway with different positions.

H(m)	σ_H(MPa)	σ^0_H (MPa)
10	23.09	14.69
20	23.08	14.94
40	22.96	15.45
60	22.66	15.96
80	22.16	16.47
100	21.49	16.98
120	20.69	17.49
140	19.81	18.00
160	18.90	18.51
180	17.99	19.02

As shown in Figure 3 and Table 1, when the vertical distance between the working face and floor roadway was less than 160 m (i.e., 0 m < $H \leq$ 160 m), the vertical stress σ_H of the surrounding rocks for the roadway always exceeded the corresponding in situ stress σ^0_H (i.e. the in situ stress of level which corresponds to different positions of the floor roadway). This indicated that the mining activities in this range affected the floor roadway and the propagation depth of the mining stress was about 160 m. When 0 m < $H \leq$ 40, the value of σ_H was greatly larger than its corresponding in situ stress σ^0_H and

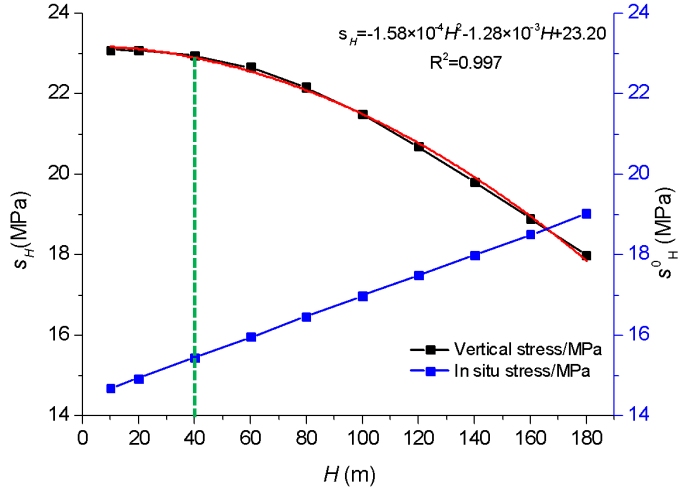

Figure 3. Vertical stress σ_H of surrounding rocks of the roadway with different positions.

maintained at about 23MPa. Moreover, the curve slope that could reflect the attenuation rate of the stress in this range was very small, so it was in the low attenuation rate state and the roadway was affected by mining activities notably due to the high stress. With an increased in H, the σ^0_H linearly increased, while the σ_H decreased when 40 m < $H \leq$ 160 m. Moreover, the attenuation rate of the vertical stress decreased notably due to the curve slope obviously increasing. Hence, the difference between σ_H and σ^0_H decreased. These indicated that the effect of mining activities on the floor roadway weakened.

The relationship between the vertical stress σ_H and vertical distance H between the working face and the floor roadway was obtained by curve fitting, as shown in Eq. (3), and a high fitting accuracy was observed. The expression was as follows:

$$\sigma_H = -1.58\times10^{-4}H^2 - 1.28\times10^{-3}H + 23.20 \quad R^2 = 0.977 \quad (3)$$

Evolution of mining stress in floors affected by overhead mining

Establishment of UDEC numerical model

The numerical simulation methods commonly used in engineering and theoretical analysis can effectively solve complex engineering problems. The UDEC is a two-dimensional discrete element calculation program for

discontinuous media that allows large deformation sliding, rotation, and detachment along the joint surface of a discrete rock mass. The structure of the overlying strata and distribution of the mining stress in the roof and floor are clearly reproduced. Thus, it satisfied the needs of the present study (Shnorhokian et al., 2014). Based on the geological conditions of panel 10302 in Xinglongzhuang coalmine, a UDEC numerical model was established with respect to the overhead mining and floor roadway.

The thicknesses of the roof and floor of panel 10302 were simplified and adjusted to satisfy the research requirements. Given the boundary effect, a 340 m (length) × 150 m (high) calculation model was established, as shown in Figure 4. The mining depth and thickness of the coal seam in the model were 500 m and 10 m, respectively. The vertical distance between the coal seam and floor roadway was 5 m, and the horizontal distance from the left boundary of the model was 150 m. In the mine-wide model, meshes were more densely discretized around the coal from which the stopes were extracted compared to those in areas near the model boundary. Thus, the discretization method made it possible to simulate the stress state in an active mining area as accurately as possible using the available computation capability (Hofmann and Scheepers, 2015; Sainoki and Mitri, 2015).

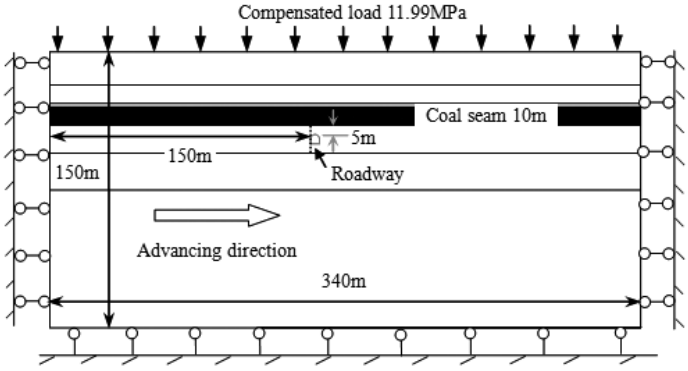

Figure 4. A numerical model for calculation.

The mechanical properties assigned to the blocks and joints of the model were conventionally derived from laboratory testing programs (Yu et al., 2016; Jiang et al., 2017b). The physical and mechanical parameters of the rock mass derived from the geological report and rock mechanical test report of the working face employed in the model were listed in Table 2. The Mohr-Coulomb model was used to simulate the continuous part of the rock because of the elastic and plastic deformation of the overlying strata, and the joint surface contact–Coulomb slip model was used to simulate the joint calculation (Itasca, 2005; Sainoki and Mitri, 2014).

The full displacement constraint boundary was used at the bottom of the model, and the horizontal displacement constraint and vertical displacement free conditions were used at the left and right sides, respectively. The top corresponded to a free boundary. The simulated depth of the coal seam was 500 m, and the roof height of the model was 30 m. Thus, the simulated failure of the overlying strata with a height of 470 m was assumed to be a result of the vertical stress that acted on the top of the numerical model. Hence, the compensated load σ_v could be calculated by Eq. (2) as follows:

$$\sigma v = \gamma h v = 25.5\text{kN/m}^3 \times 470\text{m} = 11.99\text{MPa}$$

where h_v denoted the height of the failed simulated strata. In the present study, the height of the failed simulation was set at 470 m. According to the geological report from the Xinglongzhuan coalmine, the value of the horizontal stress applied to the two sides of model with the trapezoidal distribution was half of the value of vertical stress.

Evolution of mining stress in floors affected by overhead mining

The floor roadway was significantly influenced by overhead mining within the range of 0 m < $H \leq$ 40 m, as discussed in section 2, but the effect decreased with an increase in H. Hence, in this study, based on the condition of the floor roadway located below a working face of 5 m, the laws influencing the mining stress in floor of the roadway (as affected by the overhead mining) were examined. The horizontal distance between the working face and floor roadway was defined as L_D, corresponding to 60 m, 40 m, 20 m, 0 m, -20 m and -60 m (where the negative value indicates the working face had passed the roadway) as shown in Figures 5 – 10.

Abutment stress was not only concentrated in front of the coal wall, but also would transfer to the bottom of coal floor affected by mining activities. As shown in Figures 5 and 6, when the horizontal distance between the working face and floor roadway were 60 m and 40 m (i.e., L_D = 60 m, 40m), the abutment stress was formed ahead of coal wall with 56 m and 47 m, respectively. However, the floor roadway was beyond this range when L_D = 60 m which indicated that it was not affected by overhead mining; thus the surrounding rocks of floor roadway did not fail. When L_D =40 m, the floor roadway was in the margin of the abutment stress-affected zone with the small stress concentration factor which reflected the degree of stress concentration (stress concentration factor was the ratio of concentration stress to in situ stress); thus, only the roadway roof failed. Hence, it indicated that the effect of overhead mining on the floor roadway was slight and the roadway support did not need to be strengthened when $L_D \geq 40$ m.

From Figures 7 and 8, as the working face gradually approaching the roadway, the effect of overhead mining on the roadway enhanced and the floor roadway was located in the stress significant influence area with a high-stress concentration factor of 1.6; thereby the surrounding rocks of roadways seriously destroyed, and plastic failure distributed around the roadway. Hence, when 40m>L_D≥0 m, the effect of overhead mining on the floor roadway enhanced notably by the high concentration stress and the roadway support should be paid more attention to.

From Figure 9, when 0 m>L_D≥-20 m (the negative value indicated that the working face had passed the floor roadway), the working face was passing through the roadway and the roadway was beneath the goaf of the working face; thereby locating in a stress-relaxed zone with a small stress concentration factor of 0.2 when L_D=-20 m. It meant that the effect of overhead mining on the floor roadway decreased gradually due to the small vertical stress. However, during this progress of mining operation, the roadway had experienced the effect of

Table 2. Mechanical properties of the rock mass.

Lithology	Thickness (m)	Density (Kg.m^{-3})	Bulk (GPa)	Shear (GPa)	Poisson ratio	Tensile strength (MPa)	Friction angle (º)
Siltstone	18	2530	1.34	0.76	0.2	3.08	37
Medium sand	10	2520	1.83	1.15	0.18	7.00	41
Mudstone	2	2450	0.98	0.71	0.24	1.80	31
Coal seam	10	1350	1.05	0.65	0.28	1.50	20
Siltstone	15	2530	1.34	0.76	0.28	3.08	37
Medium sand	20	2520	1.83	1.15	0.18	7.00	41
Mudstone	75	2340	0.98	0.71	0.24	1.80	31

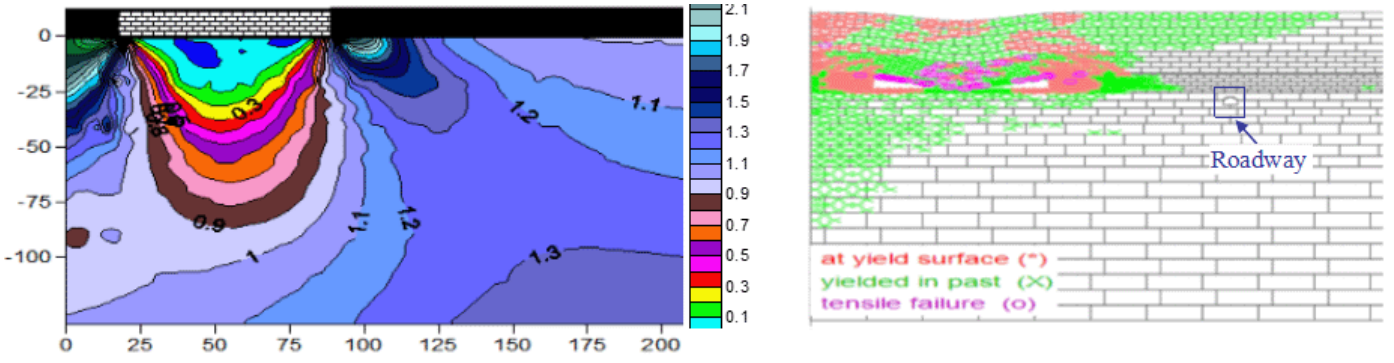

(a) (b)

Figure 5. Floor stress affected by overhead mining when L_D = 60 m: (a) Distribution of floor stress; (b) plastic zone of coal roof and floor.

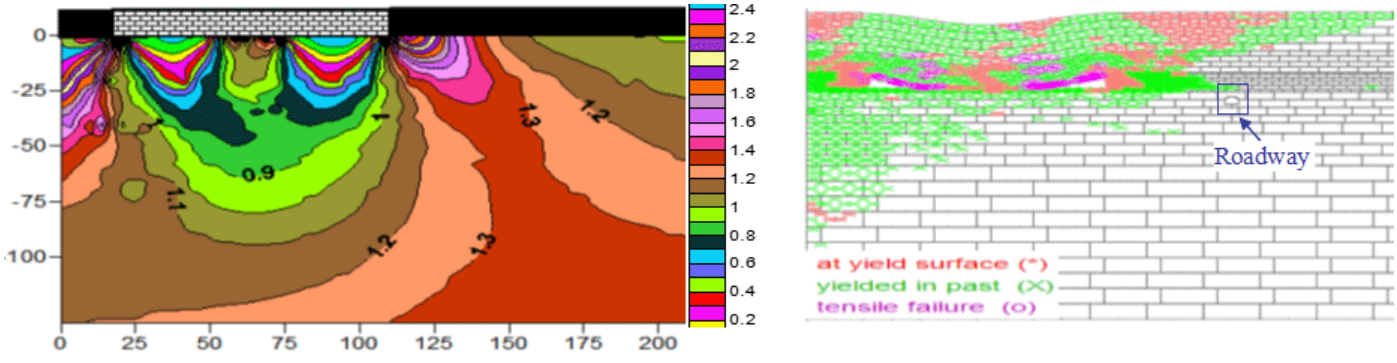

(a) (b)

Figure 6. Floor stress affected by overhead mining when L_D = 40 m: (a) Distribution of floor stress; (b) plastic zone of coal roof and floor.

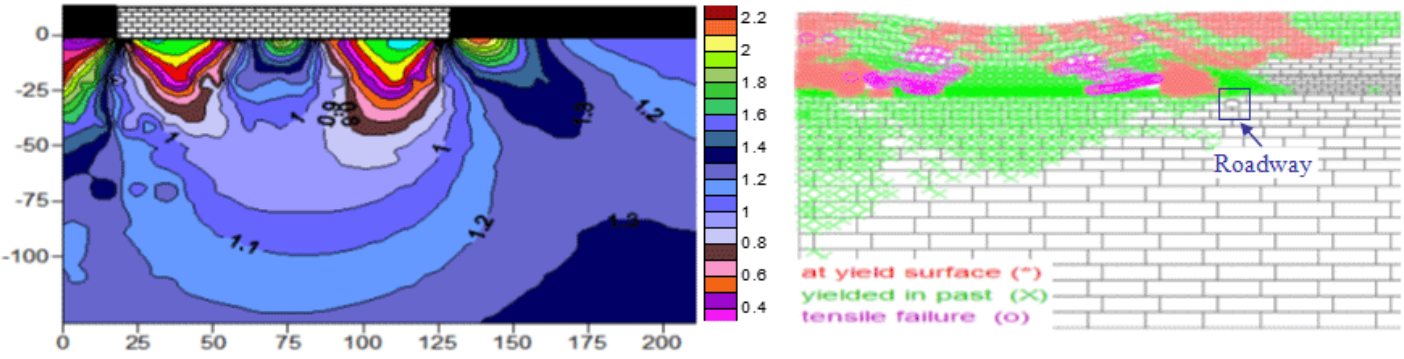

(a) (b)

Figure 7. Floor stress affected by overhead mining when L_D = 20 m: (a) Distribution of floor stress; (b) plastic zone of coal roof and floor.

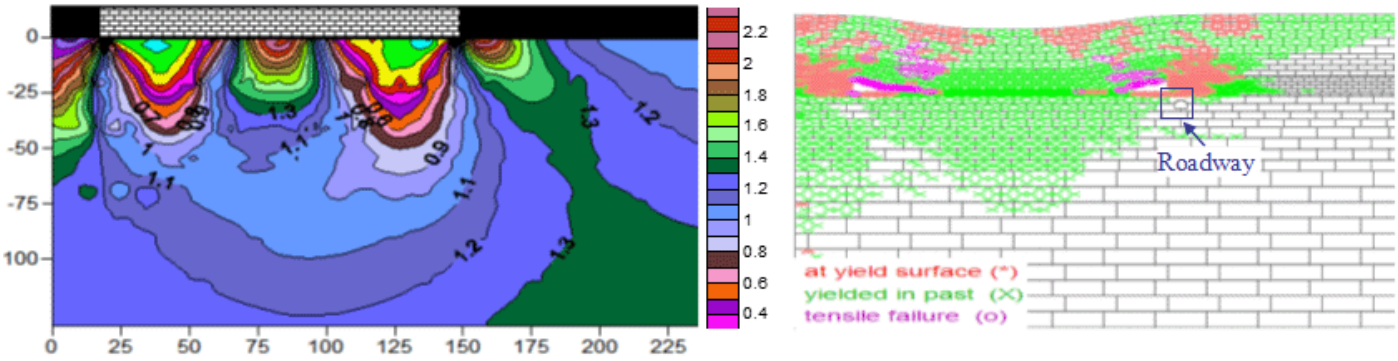

(a) (b)

Figure 8. Floor stress affected by overhead mining when L_D = 0 m: (a) Distribution of floor stress; (b) plastic zone of coal roof and floor.

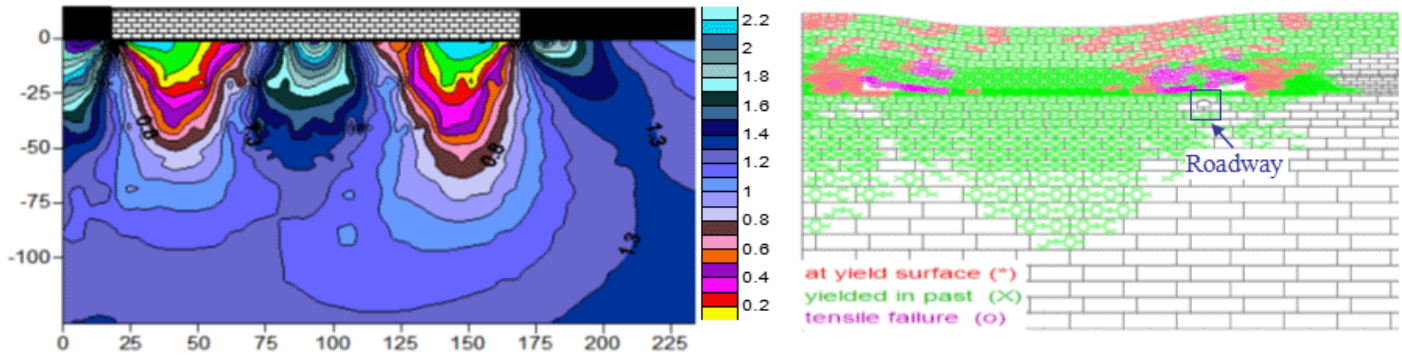

(a) (b)

Figure 9. Floor stress affected by overhead mining when L_D = -20 m: (a) Distribution of floor stress; (b) plastic zone of coal roof and floor.

the largest stress and then the effect decreased with the stress dropping; thereby inducing serious failure of surrounding rocks of roadway. Hence, in this stage, even though the roadway located in the goaf-affected zone gradually, it had experienced the notable effect of the largest stress, hence the serious failure was observed and the range of plastic failure increased as shown in Figure 9(b).

As shown in Figure 10, when -20 m>L_D≥-60 m, as the goaf zone increased, the vertical stress in the goaf recovered and increased with constant compaction of migrated overlying strata. The effect of the stress on the floor roadway increased gradually and the stress concentration factor increased to 1.2 which indicated the floor roadway re-located in the stress increasing zone when L_D=-60 m. Hence, the vertical stress in the goaf re-affected the roadway. This effect by the vertical stress in recovery zone of the goaf was often neglected although it might influence the roadway significantly, the failure of surrounding rocks of roadway aggravated again as shown in Figure 10(b). Hence, when -20 m>L_D≥-60 m, the roadway was affected by the recovered stress in the goaf and the failure of roadway aggravated further which indicated that the effect of the recovered stress on the roadway should not be ignored and necessary support should be considered with respect to the roadway.

Hence, according to the aforementioned analysis, the evolution laws of the vertical stress and the effect on the floor roadway were obtained, as shown in Table 3 and Figure 11.

The entire process of overhead mining with respect to the effect on the floor roadway was divided into four stages.

Stage I: 40 m ≤ L_D ≤ 60 m. The stress concentration factor of the rocks surrounding the roadway exceeded 1 and rose slightly with a decrease in L_D. Hence, the effect of overhead mining on the floor roadway was slight and the roadway did not need strengthened support.

Stage II: 0 m ≤ L_D < 40 m. The stress concentration factor of the rocks surrounding the roadway significantly increased and tended to be stable with a decreased in L_D, and the maximum value increased to 1.6. Hence, the effect of overhead mining on the floor roadway enhanced notably affected by high concentration stress and the roadway support should be paid more attention to.

Table 3. Stress concentration factor of rocks surrounding of floor roadway.

L_D(m)	Stress concentration factor
60	1
40	1.2
20	1.6
0	1.6
-20	0.2
-40	0.3
-60	1.2

Stage III: -20 m ≤ L_D < 0 m. The roadway was in the stress-relaxed state and the stress concentration factor significantly decreased with the working face passing through the roadway. However, it had experienced the notable effect of the largest stress during this stage, hence the serious failure of roadway was observed and the range of plastic failure increased. Thus the floor roadway support should be more strengthened.

Stage IV: -60 m ≤ L_D < -20 m. The abutment stress in the goaf corresponded to recovery and increased with the constant compaction of the migrated overlying strata. The floor roadway re-located in the stress increasing zone. Hence, the roadway was affected by the recovered stress in the goaf and the failure of roadway aggravated further which indicated that the effect of the recovered stress on the roadway should not be ignored and necessary support should be considered with respect to the roadway.

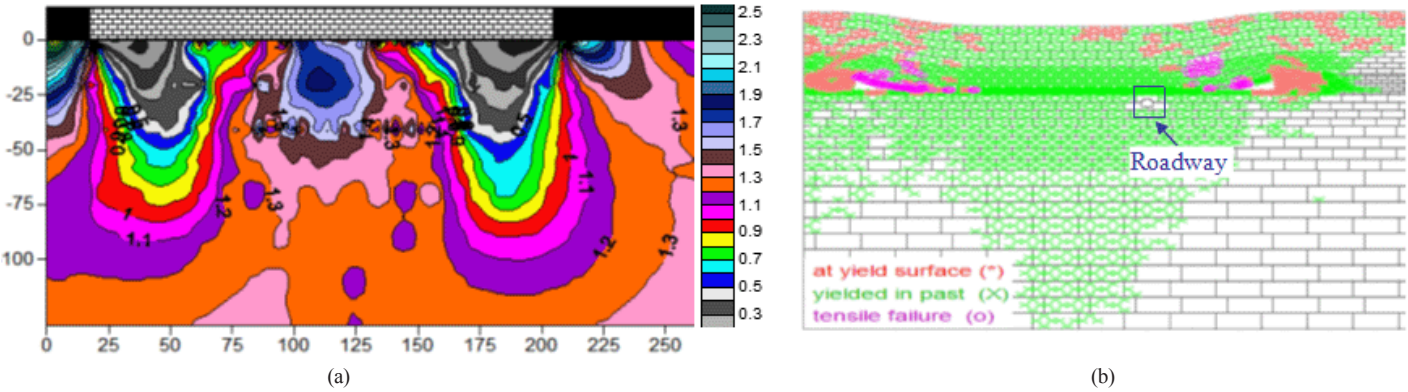

(a) (b)

Figure 10. Floor stress affected by overhead mining when L_D = -60 m: (a) Distribution of floor stress; (b) plastic zone of coal roof and floor.

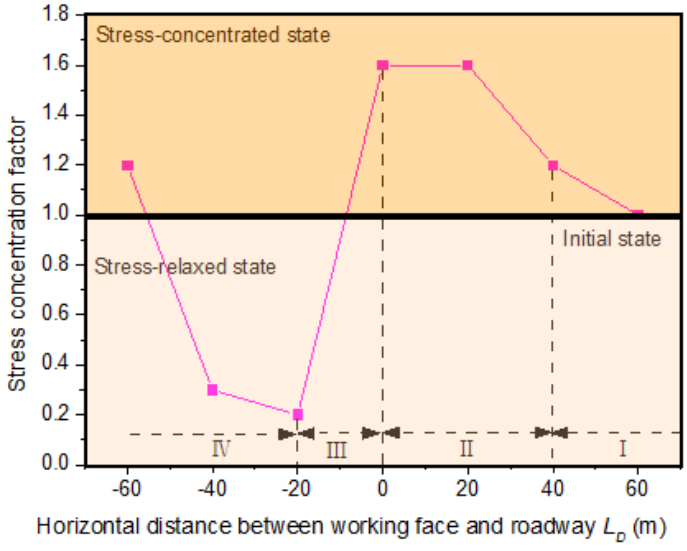

Figure 11. Relationship between L_D and stress concentration factor.

Engineering case

A significant effect of overhead mining on the floor roadway was observed in the above analysis of the theory and numerical simulation. Hence, on-site observations of the deformation and failure of a drainage roadway in Xinglongzhuang coalmine were used to verify the previously mentioned results.

Deformation monitoring of roadway.

In this study, the deformation monitoring of the roadway mainly included the relative displacement of roof to floor, which reflected the vertical deformation, and the relative displacement of two ribs, which represented the horizontal deformation. Hence, seven sections of the roadway (marked as 1–7), which corresponding positions were shown in Figure 12, were surveyed at 30 m intervals along the roadway with the mining range of 300 m. Make a sectional plane at the midpoint of working face, and obtain the three states between the working face and the floor roadway, including ahead of floor roadway, right above floor roadway and rear of floor roadway, as shown in Figure 13. Figure 14a shows the the monitoring points of surrounding rock deformation for the roadway section.

Table 4 and Figure 14 showed the final results of deformation survey for the floor roadway within the mining range of 300 m when the working face had passed through the roadway and the roadway was no longer affected by mining operation. Hence, it can be seen the vertical and horizontal deformations of the drainage roadway in sections 1–4 were large, with both values approximately 1100–1300 mm. This was because the roadway in this testing range was notably affected by the highly vertical stress of panel 10302 mining, and a large-scale plastic failure zone was formed in the rocks surrounding the

Table 4. Results of roadway deformation.

Sequence of sections	Relative displacement of roof to floor convergence (mm)	Relative displacement of two ribs convergence (mm)
No.1	1156	1203
No.2	1321	1078
No.3	1210	1135
No.4	1098	1254
Average value	1196	1167
No.5	701	743
No.6	621	703
No.7	598	664
Average value	640	703

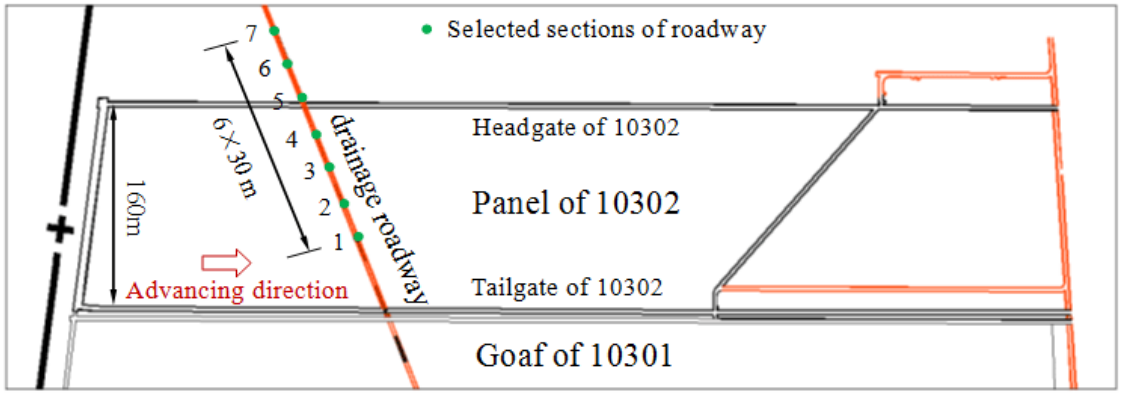

Figure 12. Plan of panel 10302 and the layout of roadway sections.

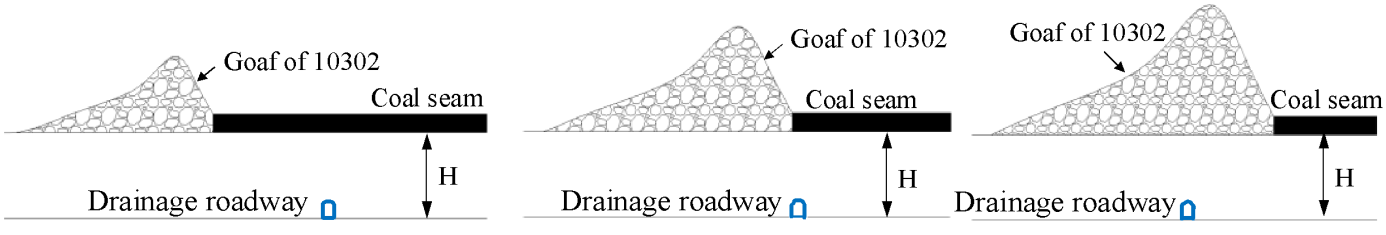

(a) Ahead of roadway (b) Right above roadway (c) Rear of roadway

Figure 13. Three states related the working face and the floor roadway.

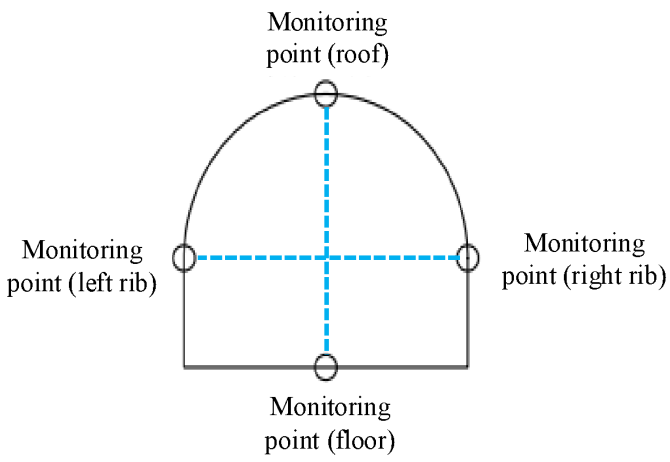

(a) Layout of monitoring points

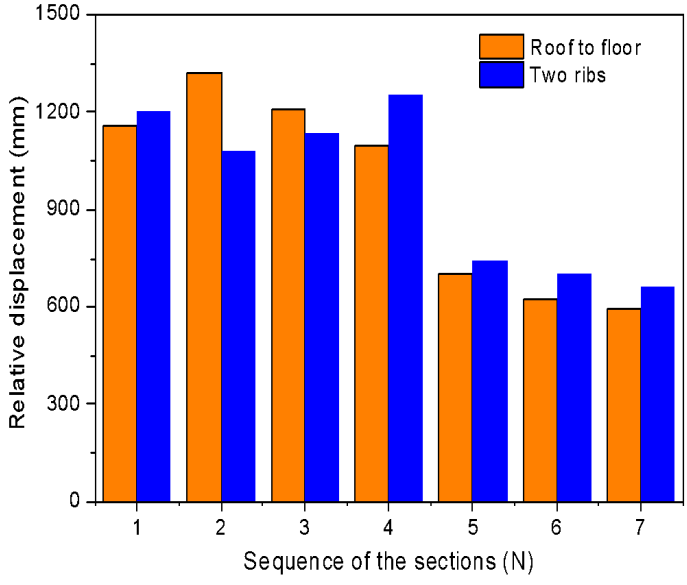

(b) Deformation of roadway

Figure 14. Results of roadway deformation.

roadway. Thus, the strength of the surrounding rocks decreased, and large deformation was observed in the roadway. Moreover, many fractures formed in the floor strata because of the mining activities. This resulted in seepage from the goaf penetrating the floor, which further reduced the strength of the surrounding rocks. However, the deformations of sections 5–7 were relatively small, with values of 600–700 mm. According to the geological report for the Xinglongzhuang coal mine, this testing range (sections 5–7) was affected by mining activities slightly compared to that of sections 1–4, and the deformation was mainly contributed by the weakening effect of the seepage from the goaf. Thus, the deformations in sections 5–7 were much smaller than those of sections 1–4. Hence, it can be concluded that the effect of overhead mining on the floor roadway was significant, and the deformation of the surrounding rocks increased notably. So this exploitation is not safe and the support for the roadway should be strengthened.

In order to study the relationship between the roadway deformation and the mining activities in detail, section 2 which was notably affected by mining were selected; and then the deformation of roof-floor and two ribs with the mining range of 300 m was surveyed. Figure 15 showed the variation curves of deformation for the roadway with mining activities.

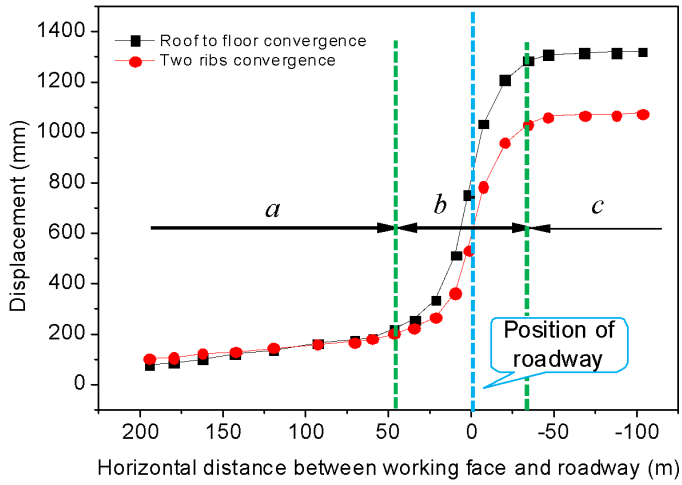

Figure 15. Deformations of section 2 of roadway with the working face mining.

As can be seen from Figure 15, the variations of roof-floor convergence and two ribs convergence of section 2 were similar and showed obvious stage characteristics during the face progress.

When the horizontal distance between working face and floor roadway exceeds 47 m, the roadway was affected by mining activities slightly, so both the roof-floor convergence and two ribs convergence were small and had no much change, as shown in Figure 15 with stage (a), which the pressure appearance from the filed observation was similar to the simulation results with 40 m $\leq L_D \leq$ 60 m in section 3.2.

When the horizontal distance between working face and floor roadway was in range of -34 m ~ 47m (the negative value indicated that the working face had passed the floor roadway), the deformation of roadway occurred significantly due to the violet effect of mining activation, resulting in both the displacement of rib-floor and two ribs convergence increasing sharply, as shown in Figure 15 with stage (b). Hence, compared with the fore-mention numerical simulation, the pressure appearance of filed observation was similar to the simulation results with -20 m $\leq L_D <$ 40 m in section 3.2.

When the working face passed through the floor roadway exceeds 34 m, the floor roadway was under the goaf of panel 10302, and the effect of mining operations on the roadway reduced gradually where roadway failure was no longer aggravated. Hence, both the roof-floor convergence and two ribs convergence rose slightly and tended to be stable, as shown in Figure 12 with stage (c). However, the both displacements were large and peak values in survey range were 1321 mm and 1078 mm (shown in Table 4) respectively. At this stage, the pressure appearance of filed observation was similar to the simulation results with -60 m $\leq L_D <$ -20 m in section 3.2.

Pull-out test analysis of bolts.

Based on the stress characteristics of the bolts, it was possible to assess the stability of the surrounding rock and the rationality of the bolt support of the roadway. Hence, pull-out tests of the existing bolts used for the drainage roadway were performed using a pull-out device (ZY-30), in which the maximum pull-out force was 300 kN. Three bolts (distributed in the roof and two ribs) were arranged in each section for the test, as shown in Figure 16a. The results of the pull-out tests are shown in Table 5 and Figure 16b.

As shown in Table 5 and Figure 16, the pull-out force for most of the bolts was unable to satisfy the minimum requirement of 50 kN as indicated in the geological report of Xinglongzhuan coalmine. The qualified rates for the bolts in the roof and two ribs corresponded to 42.9%, 28.6%, and 42.9%, respectively, with an average value of only 38.1%. This indicated that the existing support of the roadway had a poor performance during the overhead mining of panel 10302. Based on the study of Lu et al. (1998), an important reason for a low bolt pull-out force was an inability to fully utilize the anchoring capacity of the bolt system (i.e., in fractured surrounding rock, the existence of more cracks lead to bolt failure) or the existence of serious damage to the surrounding

Table 5. Results of the pull-out tests.

Sequence of sections	The pull-out force of roof (kN)	The pull-out force of left rib (kN)	The pull-out force of right rib (kN)	Note: Disqualification position
1	46	54	74	roof
2	52	28	38	two ribs
3	39	45	28	roof and right rib
4	36	61	53	roof
5	52	54	32	right rib
6	29	33	61	roof and left rib
7	51	41	28	two ribs
Qualified rate	42.9 %	28.6 %	42.9 %	Average: 38.1 %

rock, which prevented the bolt from reaching its anchorage capacity. However, according to the results of the roadway deformation monitoring, the overhead mining of panel 10302 significantly affected the floor roadway, many fractures formed in floor strata, and the deformation of the surrounding rocks increased notably. The strength of the surrounding rocks decreased. Hence, the bolts might not have fully reached their anchoring capacity as a result of the overhead mining, which produced a low pull-out force for the bolts.

Thus, the on-site results for the surrounding rock deformation and the pull-out tests of the existing bolts of the drainage roadway indicated that the floor roadway was affected by overhead mining significantly and its deformation-failure were serious; thus more attention should be paid on the similar coal measures strata. Additionally, the observation results and the numerical simulation results showed a good agreement which can further explain rationality of numerical model.

Conclusions

In this study, the laws influencing the mining-induced stress in different position of a roadway and the evolution of the mining-induced stress in floor with different horizontal distances between the working face and the floor roadway were examined to investigate the influence of overhead mining on a floor roadway. A mechanical model of a working face for overhead mining over a roadway was established, and a numerical model was generated using UDEC software.

It was found that the depth influencing the mining stress on the floor corresponded to 160 m. Thus, the mining stress was high and slowly decreased within a range of less than 40 m, through which the floor roadway was significantly affected, while the stress significantly decreased within a range exceeding 40 m, through which the effect of the stress on the roadway evidently decreased. The mining stress on the floor gradually increased, which led to an increase in the failure of the rocks surrounding the floor roadway within 0 m $\leq L_D \leq$ 60 m, and the effect was particularly evident in a range of 0 m $\leq L_D \leq$ 40 m. Although the floor roadway was in a stress-relaxed state, the worse stability of the surrounding rock was observed in a range of -20 m $\leq L_D <$ 0 m. The floor roadway was affected by the recovery of the abutment stress in the goaf when -60 m $\leq L_D <$ 20 m, and thus attention should be focused on strengthening the support. Finally, the surrounding rock deformation and bolts pull-out tests of a drainage roadway in Xinglongzhuang coalmine were used to verify the results of the numerical simulation.

The results could be utilized to serve as a scientific basis for floor roadway selection, which was affected by overhead mining in the Xinglongzhuang coalmine or its surrounding coal mines and might also provide some roadway support experience and supporting parameters for similar coal measures strata.

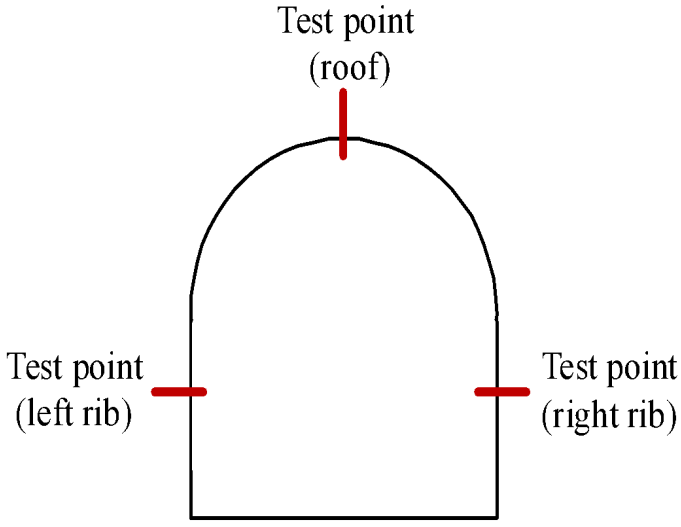

(a) Layout of test points

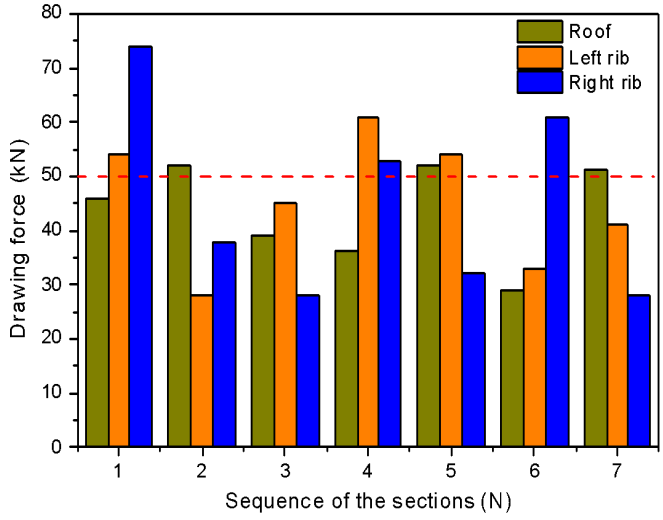

(b) Results of the pull-out tests of the bolts

Figure 16. Layout of test points and results of the pull-out tests of the bolts.

Acknowledgments:

This study was funded by the National Natural Science Foundation of China (no. 51574155, no. 51504145, no. 51704182 and no. 51704185), the Natural Science Foundation of Shandong Province (no. ZR2017BEE050 and no. ZR2017BEE045), the Shandong Provincial Key R&D Plan (Public Welfare Special Program) of China (no. 2017GGX20125), Scientific Research Foundation of Shandong University of Science and Technology for Recruited Talents (no. 2015RCJJ057), Tai'an Science and Technology Development Plan of Shandong Province (no. 2015ZC1058), Science and Technology Innovation Fund of the College of the Mining and Safety Engineering, Shandong University of Science and Technology (no. KYKC17008).

References

Dai, J., Li, H., Li, F. H., & Liu, T. X. (1999). The influence of working face advancing direction on the maintenance of overhead mining. *Mine pressure and roof management*, 3–4, 190–193.

Feng, Q., Jiang, B. S., Wang, G. & Hu, C. P. (2016). Analytical solution for a circular roadway considering the transient effect of excavation unloading. *International Journal of Mining Science and Technology*, 26(4), 543–549.

Gao, F. Q., Stead, D. & Kang, H. P. (2015). Numerical simulation of squeezing failure in a coal mine roadway due to mining-induced stresses. *Rock Mechanics and Rock Engineering*, 48(4), 1635–1645.

Hofmann, G. F. & Scheepers, L. J. (2015). Simulating fault slip areas of mining induced seismic tremors using static boundary element numerical modeling. *Transactions of the Institution of Mining & Metallurgy*, 120(1), 53–64.

Islam, M. R. & Shinjo, R. (2009). Numerical simulation of stress distributions and displacements around an entry roadway with igneous intrusion and potential sources of seam gas emission of the Barapukuria coal mine, NW Bangladesh. *International Journal of Coal Geology*, 78(4), 249–262.

Itasca. (2005). *Universal Distinct Element Code User's Guide (Version 4.0)*. Itasca Consulting Group, Minneapolis, USA, 16 pp.

Jiang, L. S., Sainoki, A., Mitri, H. S., Ma, N. J., Liu, H. T. & Hao, Z. (2016). Influence of fracture-induced weakening on coal mine gateroad stability. *International Journal of Rock Mechanics & Mining Sciences*, 88, 307–317.

Jiang, L. S., Zhang, P. P., Chen, L. J., Hao, Z., Sainoki, A., Mitri, H.S. & Wang, Q.B. (2017a). Numerical Approach for Goaf-Side Entry Layout and Yield Pillar Design in Fractured Ground Conditions. Rock Mechanics and Rock Engineering, 50(11), 3049–3071.

Jiang, L. S., Wang, P., Zhang, P. P., Zheng, P. Q. & Xu, B. (2017b). Numerical analysis of the effects induced by normal faults and dip angles on rock bursts. *Comptes Rendus Mecanique*, 345(10), 690–705.

Kang, Q. R., Tang, J. X., Hai, H. U. & Zhang, W. Z. (2011). Stress distribution rule of roadway affected by overhead mining in gently inclined coal seams group. *Transactions of Nonferrous Metals Society of China*, 21(S3), 529–535.

Li, G. C. (2011). Study on the surrounding rock stability and safety control of roadways roof embedded weak intercalated seam. Ph.D. thesis, China University of Mining and Technology, Beijing, China.

Li, Q. H., Shi, W. P. & Qin, Z. C. (2016). Effect of bolting on roadway support in extremely weak rock. *SpringerPlus*, 5(1), 1355–1372.

Li, Y. Y. (2011). Study on the technology of surrounding rock control in floor roadway under repeated overhead mining. Ph.D. thesis, China University of Mining and Technology, Beijing, China.

Liu, X. J., Li, X. M. & Pan, W. D. (2016). Analysis on the floor stress distribution and roadway position in the close distance coal seams. *Arabian Journal of Geosciences*, 9(2), 1–8.

Liu, C., Li, S. G., Cheng, C. & Cheng, X. Y. (2017). Identification methods for anomalous stress region in coal roadways based on microseismic information and numerical simulation. *International Journal of Mining Science and Technology*, 27(3), 525–530.

Lu, H. F., Yao, D. X., Hu, Y. B., Sun, J. (2017). Elasticity solution for failure depth of mining floor under water pressure. *Journal of Mining & Safety Engineering*, 34(3), 452–458.

Lu, S. L., Tang, L., Yang, X. A. (1998). *Anchorage force of bolts and anchorage technology*.China Coal Industry Publishing House, Beijing, 34p.

Ma, R., Li, G. C., Zhang, N., Liu, C., Wei, Y. H. & Zhang, M. (2015). Analysis on mechanism and key factors of surrounding rock instability in deeply inclined roadway affected by argillation and water seepage. *International Journal of Mining Science and Technology*, 25(3), 465–471.

Sainoki, A. & Mitri, H. S. (2015) Evaluation of fault-slip potential due to shearing of fault asperities. *Canadian Geotechnical Journal*, 52, 1417–1425.

Sainoki, A. & Mitri, H. S. (2014b). Dynamic modelling of fault-slip with Barton's shear strength model. *International Journal of Rock Mechanics & Mining Sciences*, 67(6), 155–163.

Shnorhokian, S., Mitri, H. S. & Thibodeau, D. (2014). Numerical simulation of pre-mining stress field in a heterogeneous rockmass. *International Journal of Rock Mechanics & Mining Sciences,* 66(9), 13–18.

Wang, B., Liu, S. D., Zhou, F. B., Zhang, J. & Zheng, F. K. (2017). Diffraction characteristics of small fault ahead of tunnel face in coal roadway. *Earth Sciences Research Journal,* 21(2), 95–99.

Wang, F. T., Duan, C. H., Tu, S. H., Liang, N. N. & Bai, Q. S. (2017). Hydraulic support crushed mechanism for the shallow seam mining face under the roadway pillars of room mining goaf. *International Journal of Mining Science and Technology*, 27(5), 853–860.

Wang, P., Jiang, L. S., Jiang, J. Q., Zheng, P. Q. & Li, W. (2018). Strata behaviors and rock burst-inducing mechanism under the coupling effect of a hard, thick stratum and a normal fault. *International Journal of Geomechanics*, 18(2), 04017135.

Wang, W., Cheng, Y. P., Wang, H.F., Liu, H. Y., Wang, L., Li, W. & Jiang, J. Y. (2015). Fracture failure analysis of hard-thick sandstone roof and its controlling effect on gas emission in underground ultra-thick coal extraction. *Engineering Failure Analysis*, 54, 150–162.

Yin, H. F., Wang, H. & Zhu, H. X. (1992). Applying the space elastic theory to analyse and compute the stress distribution in the floor affected by extract. *Journal of Fuxin Mining Institute*, 11(1), 19–24.

Yu, B., Zhao, J., Fang, K., Tan, Y. L. & Ning, J. G. (2016). Rock strength evaluation during progressive failure process based on fractural characterization. *Marine Georesources & Geotechnology*, 34(8), 1–5.

Yuan, A. Y., Yang, Z. Y. & Yang, Y. M. (2016). Across mechanical analysis and control technology of surrounding rock of roadway under the influence of dynamic pressure. *Metal Mine*, 45(2), 47–50.